



## Chemoorganotrophic electrofermentation by *Cupriavidus necator* using redox mediators

André Gemünde<sup>a,1</sup>, Elena Rossini<sup>b,1</sup>, Oliver Lenz<sup>b</sup>, Stefan Frielingsdorf<sup>b,\*</sup>, Dirk Holtmann<sup>a,c,\*</sup>

<sup>a</sup> Institute of Bioprocess Engineering and Pharmaceutical Technology and Competence Centre for Sustainable Engineering and Environmental Systems, University of Applied Sciences Mittelhessen, 35390 Giessen, Germany

<sup>b</sup> Institute of Chemistry, Biophysical Chemistry, Technische Universität Berlin, Straße des 17. Juni 135, 10623 Berlin, Germany

<sup>c</sup> Institute of Process Engineering in Life Sciences, Karlsruhe Institute of Technology, Kaiserstraße 12, 76131 Karlsruhe, Germany

### ARTICLE INFO

#### Keywords:

*Cupriavidus necator*  
Bioelectrochemical systems  
Redox mediators  
Biocompatibility  
Anodic respiration

### ABSTRACT

The non-pathogenic  $\beta$ -proteobacterium *Cupriavidus necator* has the ability to switch between chemoorganotrophic, chemolithoautotrophic and electrotrophic growth modes, making this microorganism a widely used host for cellular bioprocesses. Oxygen usually acts as the terminal electron acceptor in all growth modes. However, several challenges are associated with aeration, such as foam formation, oxygen supply costs, and the formation of an explosive gas mixture in chemolithoautotrophic cultivation with  $H_2$ ,  $CO_2$  and  $O_2$ . Bioelectrochemical systems in which  $O_2$  is replaced by an electrode as a terminal electron acceptor offer a promising solution to these problems. The aim of this study was to establish a mediated electron transfer between the anode and the metabolism of living cells, i.e. anodic respiration, using fructose as electron and carbon source. Since *C. necator* is not able to transfer electrons directly to an electrode, redox mediators are required for this process. Based on previous observations on the extracellular electron transfer enabled by a polymeric mediator, we tested 11 common biological and non-biological redox mediators for their functionality and inhibitory effect for anodic electron transfer in a *C. necator*-based bioelectrochemical system. The use of ferricyanide at a concentration of 15 mM resulted in the highest current density of  $260.75 \mu A cm^{-2}$  and a coulombic efficiency of 64.1 %.

### 1. Introduction

Biotechnological processes are becoming increasingly efficient and used in various industries, e.g. pharmaceuticals, wastewater treatment, synthesis of fine and base chemicals, and energy production [1–3]. For these processes, highly efficient microorganisms are a key element to be economically viable. Among those organisms, *Cupriavidus necator* (formerly *Ralstonia eutropha*) is demonstrating promise as a production strain for several reasons. This Gram-negative, strictly respiratory  $\beta$ -proteobacterium possesses the ability to utilize a wide range of carbon sources such as fructose, organic acids, and glycerol in chemoorganotrophic cultivation [4]. Furthermore, chemolithoautotrophic cultivation of *C. necator* with “Knallgas” ( $H_2/O_2$ ) and  $CO_2$  as feedstock

can be exploited to produce valuable compounds such as  $\alpha$ -humulene [5] and biopolymers such as polyhydroxybutyrate (PHB) [6]. In addition, *C. necator* is genetically amenable and appropriate genetic tools are available [7,8].

A “Knallgas” mixture in conjunction with  $CO_2$  represents a simple and inexpensive feedstock, but can pose a significant explosion risk in (large-scale) fermenters. Bioelectrochemical systems in which  $O_2$  is replaced by an electrode as terminal electron acceptor offer a promising solution to this problem [9–11]. Such systems could overcome the limitations associated with  $O_2$  solubility and transfer while preventing excessive foaming due to aeration. Moreover, using an electrode as the terminal electron acceptor provides an inexhaustible electron sink, which distinguishes it from molecular electron acceptors in general

**Abbreviations:** DCIP, 2,6-dichloroindophenole; DHB, 3,4-dihydroxybenzaldehyde; DPV, differential pulse voltammetry; FEC, ferricyanide; HNQ, 2-hydroxy-1, 4-naphthaquinone; MB, methylene blue; MV, methyl viologen; PES, phenazine ethosulfate; PMS, phenazine methosulfate; RES, resazurin; RF, riboflavin; RM, redox mediator.

\* Corresponding authors at: Institute of Process Engineering in Life Sciences, Karlsruhe Institute of Technology, Kaiserstraße 12, 76131 Karlsruhe, Germany (D. Holtmann); Institute of Chemistry, Biophysical Chemistry, Technische Universität Berlin, Straße des 17. Juni 135, 10623 Berlin, Germany (S. Frielingsdorf).

E-mail addresses: [stefan.frielingsdorf@tu-berlin.de](mailto:stefan.frielingsdorf@tu-berlin.de) (S. Frielingsdorf), [dirk.holtmann@kit.edu](mailto:dirk.holtmann@kit.edu) (D. Holtmann).

<sup>1</sup> These two authors contributed equally to this work.

<https://doi.org/10.1016/j.bioelechem.2024.108694>

Received 3 November 2023; Received in revised form 13 March 2024; Accepted 16 March 2024

Available online 18 March 2024

1567-5394/© 2024 The Authors. Published by Elsevier B.V. This is an open access article under the CC BY license (<http://creativecommons.org/licenses/by/4.0/>).

[10]. Microorganisms require an efficient electron transfer mechanism that overcomes the non-conductive cell membranes. This so-called extracellular electron transfer (EET) to and from an electrode can occur via three principal routes. First, certain microorganisms are able to attach directly to the electrode surface and can reversibly transfer electrons between the electrode and the cell via a chain of redox-active proteins that electronically connect the outer membrane and the cytoplasmic membrane. This mechanism is referred to as direct electron transfer (DET) and only happens when cells are in the immediate vicinity of the electrode surface and synthesize special redox-active proteins. *Geobacter sulfurreducens* and *Shewanella oneidensis*, for example, employ this mechanism for the dissimilatory reduction of solid Fe(III) [12,13]. The other two possibilities involve soluble molecular redox shuttles that do not necessarily require outer membrane cytochromes. These can be molecules that are produced by the electrode or the organism and are oxidized/reduced only once (indirect electron transfer, IET). This includes, for example, the electrochemical production of H<sub>2</sub> or O<sub>2</sub>, which *C. necator* can then use as electron donor/acceptor [5]. On the other hand, shuttle molecules can be used that can undergo multiple redox cycles and mediate the electron exchange between electrode and organism (mediated electron transfer, MET). Here, shuttle-based electron transfer is not limited to the confined electrode surface, but can occur throughout the entire volume of the bioreactor. Some of these mediators can be produced endogenously by the microorganisms enabling a constant supply of the shuttle molecule [14]. The addition of artificial redox mediators to the culture medium can either support these natural shuttles or enable EET in a non-electrogenic microorganism such as *Pseudomonas putida* [15].

A variety of redox mediators (RM) offer the possibility of facilitating EET between living organisms and an electrode. However, their selection must be carefully made based on factors such as redox potential, molecular interaction site, inhibitory effects, and membrane permeability [16]. Monitoring chromatic properties of the RMs using UV-vis in the bioreactor allows a rapid assessment of the redox properties of the different RMs *in situ* and provides insight on their suitability for efficient microorganism-mediator interaction [15].

Proficient electronic extracellular interaction of *C. necator* with RMs has already been demonstrated. For example, *C. necator* cultures grown on 10 mM fructose showed enhanced aerobic PHB production in the presence the RM poly(2-methacryloyloxyethyl phosphorylcholine-co-vinylferrocene) recycled from an anode [17]. Nevertheless, the achieved current density of ca. 6.5  $\mu\text{A cm}^{-2}$  was very low, since O<sub>2</sub> was introduced as additional electron acceptor into the working electrode chamber. In another approach using neutral red as RM and an applied current of 10 mA, the PHB yield in a bioelectrochemical system (BES) has been increased by cathodic supplementation of electrons [18]. Furthermore, chemolithoautotrophic photo-electro-cultivation has recently been demonstrated by the addition of riboflavin, in which a cathode acts as the sole electron donor [19]. This was even further enhanced in a recent publication by Tu and co-workers [20]. Here, the authors implemented the Mtr electron transfer pathway from *S. oneidensis* together with a *Gloeobacter* rhodopsin. The rhodopsin hereby ensures a proton motive force while the Mtr pathway supplies electrons for NAD reduction to drive CO<sub>2</sub> fixation to biomass. Additionally, flavins have been artificially added to further facilitate the electron transfer. However, “anodic respiration”, describing the anode acting as a terminal electron acceptor, in the absence of O<sub>2</sub> to mitigate explosion risks of “Knallgas”-fermentation has not yet been demonstrated.

Recent advances suggest that artificial DET may be possible for *C. necator* by introducing conductive pili or flagella-like structures whose conductive properties have been enhanced by increasing their aromaticity [21]. Although this might be a promising strategy, it has been described that *C. necator* is unable to grow stable biofilms necessary for DET [22]. RMs can circumvent this problem since MET does not require biofilm formation.

Anodic respiration in *C. necator* has not been reported so far, and

many RMs, including ferricyanide, phenazine methosulfate, or pyocyanin, cannot be added to the cell culture in large quantities because of their inhibitory effect on microorganisms [23,24]. To investigate the applicability of available RMs to *C. necator*, 11 RMs with different redox potentials were characterized in this study for their inhibitory effects on growing *C. necator* cultures. Since the anodic electron transfer should not depend on the type of electron donor and limitations of mass transfer by poorly soluble gases are undesirable, fructose was used as substrate instead of H<sub>2</sub>/CO<sub>2</sub> in this study. Four of the most promising RMs were then tested for their ability to support fructose-driven anodic respiration of *C. necator* in a BES.

## 2. Materials and methods

### 2.1. Bacterial strains and chemicals

*Cupriavidus necator* PHB<sup>4</sup> [25] was used in all biotic experiments. All chemicals used for this work were supplied by Merck KGaA (Germany), VWR Chemicals (USA), Carl Roth GmbH & Co. KG (Germany), Alfa Aesar (USA), or Sigma Aldrich (USA). The redox mediators (abbreviation, redox potential vs. SHE, purity) used in this study were methyl viologen dichloride-hydrate (MV, -440 mV, 98 %), riboflavin (RF, -208 mV, 98 %), 2-hydroxy-1,4-naphthaquinone (HNQ, -140 mV, 97 %), 1,9-Dimethyl-methylene blue (MB, 11 mV, 80 %), phenazine ethosulfate (PES, 55 mV, >95 %), resazurin sodium salt (RES, 65 mV, 74 %), phenazine methosulfate (PMS, 80 mV, >90 %), 2,6-dichloroindophenole sodium salt hydrate (DCIP, 217 mV, 99 %), 3,4-dihydroxybenzaldehyde (DHB, 402 mV, 97 %), potassium ferricyanide (FEC, 416 V, >98 %), 2,2'-azino-bis(3-ethylbenzothiazoline-6-sulfonic acid) diammonium salt (ABTS, 668 mV, 98 %), neutral red sodium salt (NR, -325 mV, >90 %), methyl red sodium salt (MR, 370 mV, 99 %), and menadione (MEN, 30 mV, >98 %) [26–29].

### 2.2. Media and culture conditions

*C. necator* precultures grew in 2.5 mL LB medium (10 g L<sup>-1</sup> tryptone, 5 g L<sup>-1</sup> yeast extract, 10 g L<sup>-1</sup> NaCl) in cultivation tubes at 30 °C and 180 rpm. Cryo stocks were prepared by adding 25 % glycerol to an exponential culture and subsequent freezing at -80 °C. For BES precultures, cryo stocks were first cultivated on LB agar plates (15 g L<sup>-1</sup> agar) and incubated overnight at 30 °C. Liquid precultures were then prepared by transferring one colony into a baffled 100 mL flask containing 20 mL LB medium. After 24 h, baffled 1 L shake flasks filled with 200 mL MMasy medium were inoculated with the exponential preculture to an OD<sub>600</sub> of 0.1. MMasy medium contained 4 g L<sup>-1</sup> fructose as carbon and electron source, 2.895 g L<sup>-1</sup> Na<sub>2</sub>HPO<sub>4</sub>, 2.707 g L<sup>-1</sup> NaH<sub>2</sub>PO<sub>4</sub>·H<sub>2</sub>O, 0.94 g L<sup>-1</sup> (NH<sub>4</sub>)<sub>2</sub>SO<sub>4</sub>, 0.8 g L<sup>-1</sup> MgSO<sub>4</sub>·7H<sub>2</sub>O, 0.097 g L<sup>-1</sup> CaSO<sub>4</sub>·2H<sub>2</sub>O, 0.17 g L<sup>-1</sup> K<sub>2</sub>SO<sub>4</sub>, and 0.1 % (v/v) of trace element solution. The trace element stock solution consisted of 15 g L<sup>-1</sup> FeSO<sub>4</sub>·7H<sub>2</sub>O, 2.4 g L<sup>-1</sup> MnSO<sub>4</sub>·H<sub>2</sub>O, 2.4 g L<sup>-1</sup> ZnSO<sub>4</sub>·7H<sub>2</sub>O, 0.48 g L<sup>-1</sup> CuSO<sub>4</sub>·5H<sub>2</sub>O, 1.8 g L<sup>-1</sup> Na<sub>2</sub>MoO<sub>4</sub>·2H<sub>2</sub>O, 1.5 g L<sup>-1</sup> Ni<sub>2</sub>SO<sub>4</sub>·6H<sub>2</sub>O, and 0.04 g L<sup>-1</sup> CoSO<sub>4</sub>·7H<sub>2</sub>O dissolved in 0.1 M HCl [30]. The BES precultures were then incubated in an orbital shaker at 180 rpm (2.5 cm orbit, Multitron, Infors, Bottmingen, Switzerland) for 48 h to ensure the stationary phase was reached before inoculating the reactor.

To test the impact of RM on cell growth, cells were pre-cultured in MMasy medium containing fructose for ~ 24 h until they reached optical density (OD) values of 3.5–4.5 at 600 nm. The cells were washed once with carbon-free MMasy medium and inoculated to an initial OD<sub>600</sub> of 0.5 in MMasy medium (4 g L<sup>-1</sup> fructose) for the growth experiment. Cell growth was monitored in 96-well plates (Microtiteration plates ROTILABO® F-profile, Carl Roth). Each well contained 150  $\mu\text{L}$  of MMasy medium and serial dilutions of RM. For each experiment, a control culture without RM was included. Breath-Easy® sealing membrane (Sigma-Aldrich) was used to prevent evaporation. The OD was monitored in a SPECTRAMax® 340PC microplate spectrophotometer with

constant shaking and the OD was measured every twelve minutes. To ensure the reliability of obtained OD values, the linearity of the SPEC-TRAmAx® plate reader was confirmed in the range from 0.1 to 1.5.

Interference of the RM absorbance with the OD measurements was avoided by monitoring the OD at a wavelength where the RM absorbance is minimal or absent. The wavelengths used were 470, 600, and 800 nm. In addition, solutions of each RM concentration were included in the measurements to subtract the respective blank values. Since the pathlengths of a standard cuvette (1 cm) and the plate well are different, the plate reader OD values were converted to a pathlength of 1 cm using the factors 2.93 for OD<sub>600</sub>, 2.45 for OD<sub>800</sub>, and 3.13 for OD<sub>470</sub> for the standardized representation of the growth curves. Growth curves shown represent the average of three independent experiments (n = 3). To relate RM concentration to growth rate, the ratio between growth rate in the presence and absence of mediator ( $\mu_i/\mu_0$ ) was plotted against the RM concentration.

In the dose–response graph, the IC50 indicates half the maximum inhibitory concentration of inhibitor *I* by fitting the data with an equation based on previous work [31]. Since the data was normalised to relative growth rates in the range from 0 to 1, the equation was simplified as follows (Eq. (1)). *I* is the concentration of the inhibitor (here the RM), and *b* is the factor describing the steepness of the linear part of the curve between 0 and 1.

$$\frac{\mu_i}{\mu_0} = \frac{1}{1 + \left(\frac{I}{IC50}\right)^b} \quad (1)$$

The reduction of ferricyanide (FEC) was monitored in an independent experiment by measuring absorbance at 420 nm in minimal medium containing 3.75 mM FEC inoculated with cells to an OD<sub>600</sub> of 0.5. Cell-free minimal medium containing FEC was used for the blank. The resulting absorbance values were converted to 1 cm pathlength by multiplying by a factor of 2.23.

### 2.3. Bioelectrochemical system

The BES reactor (300 mL working volume, SR0400SS, Eppendorf DASGIP, Germany) was set up as described in detail before [9] but without the sparger. Instead, 99.999 % nitrogen was purged through the reactor headspace at 45 mL min<sup>-1</sup> throughout the experiment to maintain anoxic conditions. In short, a polished graphite rod, held in place by a PTFE rod, with a length isolated to 80 mm and a diameter of 7 mm (Graphite 24, Germany) was used as working electrode in combination with a stainless-steel mesh electrode (1.4404, mesh size 0.1 mm, wire diameter 0.065 mm, Jaera GmbH + Co.KG, Germany) with a geometrical surface area of 20 cm<sup>2</sup> as a counter electrode. The anodic and cathodic compartment were separated from each other with a cation exchange membrane (Nafion117, QuinTech, Germany), while the cathodic compartment is made out of a glass tube with a thread on one side and open on the other side holding 10 mL of cathode buffer (28.95 g L<sup>-1</sup> Na<sub>2</sub>HPO<sub>4</sub>, 27.07 g L<sup>-1</sup> NaH<sub>2</sub>PO<sub>4</sub>·H<sub>2</sub>O). As anodic buffer, MMasy medium was used with 4 g L<sup>-1</sup> fructose as substrate. The applied potential was controlled via a multi-channel potentiostat (MultiEmStat3+, PalmSens, Netherlands) and Ag/AgCl (satd. KCl) reference electrodes (Xylem Analytics, Germany). Additionally, the reactors were covered in aluminium foil to exclude light-induced decomposition of the RMs. Phenazine methosulfate (PMS) and ferricyanide (FEC) were added to the reactor medium as concentrated stock solutions. 2-hydroxynaphthaquinone (HNQ) and 2,6-dichloroindophenole (DCIP) are less soluble in aqueous media and were therefore dissolved directly in the minimal medium. An anodic overpotential of approximately 200 mV above the oxidation potential of the respective RM was applied to ensure sufficient driving force for mediator oxidation, resulting in the following applied voltages: 697 mV for FEC, 497 mV for DCIP, 297 mV for PMS, and 197 mV for HNQ. The potentiostat used could not compensate for the ohmic

drop due to the resistance between the working and reference electrode. Nevertheless, the estimated resistance values of 8 to 24 Ω in each reactor, determined by double potential step amperometry, were negligibly small compared to the applied overpotential. The pH was controlled by pH sensors (Hamilton, Germany) together with Eppendorf DASGIP pH and pump modules, feeding 2.5 M NaOH through the headspace of each reactor. With this, a pH of 6.8 was kept in the anodic compartment, while the cathodic chamber is uncontrolled.

### 2.4. Analytics

Culture samples were withdrawn from the reactors and centrifuged at 16,900 x g and 4 °C for 5 min. The resulting supernatant was further filtered through a 0.2 μm PTFE filter for HPLC analysis. Fructose concentrations were determined using an Agilent 1200 high-performance liquid chromatography system in combination with an Aminex HPX-87H column (Bio-Rad Laboratories GmbH, Germany) and a refractive index detector at 32 °C. The column was heated to 50 °C, and 5 mM H<sub>2</sub>SO<sub>4</sub> at a flow rate of 0.5 mL min<sup>-1</sup> was used to isocratically elute the analytes. Fructose standards were measured at seven concentrations between 0.1 and 4 g L<sup>-1</sup>, and the corresponding peak area fitted by linear regression (Figure S1).

The cell dry weight was determined by first centrifuging the entire culture volume of the reactor at 4 °C and 3214 x g (Centrifuge 5810 R, Eppendorf, Germany). The cell pellet was washed twice in pure water to remove media components. Finally, the washed cells were weighed on a scale equipped with a heating element (KP-7291, Kern, Germany) until no water loss was measurable.

### 2.5. Mediator concentration and redox state

RM concentrations in the BES were determined by absorbance measurements as previously described [9] at wavelengths 420 and 320 nm for FEC, 383 nm for PMS, 452 nm for HNQ, and 607 nm for DCIP. Calibration was performed with 7 different concentrations at the characteristic wavelength of the respective mediator (Figure S2).

### 2.6. Electrochemical analysis and calculations

The midpoint potential ( $E_m$ ) was determined as the average of anodic and cathodic peak potentials using the equation  $E_m = (E_{ox} + E_{red})/2$ . Total mediator turnover number (TTN) and coulombic efficiency (CE) in the BES were calculated as previously described [9] with the formula  $TTN = Q_{anode}/(F \cdot M_{mediator} \cdot z_{mediator})$ . With *Q* as the total charge transferred to the anode from the inoculation until the end of the experiment in coulomb, *F* being Faraday's constant (96485.3365C mol<sup>-1</sup>), *M*<sub>mediator</sub> the absolute amount of mediator molecules in mol, and *z*<sub>mediator</sub> the number of electrons that can be transferred by the mediator in one cycle.

The uncompensated resistance ( $R_u$ ) between the working and reference electrodes of the BES reactors was determined via a double potential step chronoamperometry. Here, a potential step of 100 mV was applied after a 10 s offset polarisation. The initial current of the potential step was used to calculate the  $R_u$  via Ohm's law. Differential pulse voltammetry (DPV) was carried out in the BES reactors with 50 mV pulses for 300 ms between -800 and 600 mV vs. Ag/AgCl (saturated KCl).

## 3. Results and discussion

### 3.1. Redox mediator impact on growth

To determine the appropriate RM concentrations for the application in a BES, the impact of redox mediators on cell growth was first evaluated. The mediators were chosen based on their redox potential in the physiological range of -440 to +668 mV, which allows both cathodic electrosynthesis and anodic respiration within a BES. In this study, all

redox potentials are given against the standard hydrogen electrode (SHE). Neutral red, methylene red, and menadione could not be analysed, because of their poor solubility in aqueous solutions and, for the same reason, not more than 90  $\mu\text{M}$  of RF could be tested.

In the case of methylene blue, it was not possible to reliably determine the inhibitory concentration for growth as growth curves lack completely the lag phase typically observed, and the cultures reached an optical density (OD) of 1 in less than forty minutes, much faster than the control culture without MB (Figure S3). Interestingly, this behaviour was more pronounced with increasing MB concentrations. This could imply a benefit for the cells, e.g. through additional respiratory capacity due to MB reduction. However, since MB has been shown to be toxic for certain bacteria [32], the OD increase might even be caused by cell lysis and would thus not be based on cell number.

Initial experiments to determine if the initial OD of the culture after inoculation affects the tolerance of the cells to the RM were performed. *C. necator* cell cultures inoculated at an OD 0.5 were found to tolerate higher RM concentrations than cultures inoculated at OD 0.1. This behaviour was confirmed for FEC and DCIP but was not studied for all mediators. Cells inoculated at an initial OD of 0.5 grow vigorously in the presence of 15 mM FEC (Figure S4), whereas no growth was observed for cells inoculated at an OD of 0.1. In the case of DCIP, growth was observed for cells inoculated at an OD 0.5 in the presence of 2 mM RM, whereas significant growth was noted for cells inoculated at OD 0.1 only at 500  $\mu\text{M}$  RM (Figure S4). Based on these results, it can be assumed that for the same mediator concentration, lower cell concentrations are more affected as each cell is exposed to a larger number of mediator molecules compared to higher ODs. Hence, we decided to analyze the growth inhibition by RM at an initial OD of 0.5, since even higher cell densities should be used in BES, but cannot be tested photometrically *in situ* due to the limited linearity of the light scattering measurements.

To ensure that no substrate limitation occurred during the growth experiment, it was first examined in the plate reader which substrate concentration was sufficient by testing the fructose concentrations in minimal medium of 2 g L<sup>-1</sup>, 4 g L<sup>-1</sup>, and 8 g L<sup>-1</sup> (Figure S5). A concentration of 4 g L<sup>-1</sup> turned out to be not limiting and although 2 g L<sup>-1</sup> fructose were already sufficient to achieve an OD (at 600 nm) of 1.2, the growth experiments were carried out at a concentration of 4 g L<sup>-1</sup> fructose to comply with the medium composition developed by Sydow et al. for *C. necator* in BES [30].

In another control experiment, we checked if the redox mediators were quantitatively reduced under aerobic growth conditions. Since most reduced RMs are immediately re-oxidized by O<sub>2</sub> [33–37], ferricyanide was used for this assay, since its reduced form ferrocyanide is only slowly re-oxidized under aerobic conditions [35,38]. Therefore, the characteristic absorbance of FEC at 420 nm was used to monitor its reduction while tracking the cell density [9]. Right at the start of the experiment, a significant decrease in absorbance at 420 nm was observed (Figure S6), showing that ferricyanide was reduced by the cells even in presence of O<sub>2</sub>. Thus, the cells reduce the redox mediator in parallel with O<sub>2</sub> respiration.

The experiments on the inhibition of cell growth revealed that the presence of a RM usually affects the lag phase, growth rate, and/or the rate of reaching the stationary phase (Figure S3). Of the mediators tested, ABTS had the least impact, as the cell culture in the presence of 5 mM ABTS exhibited a lag phase and growth rate similar to that of the control. FEC, ABTS and RES were the RMs that could be used at the highest concentrations at 15 mM, 10 mM, and 10 mM, respectively. In the case of ABTS and RES, the limiting factor was their solubility in the minimal medium rather than their inhibitory effect to cells.

To better compare the relationship between mediator concentration and growth rate, relative growth rates  $\mu_i/\mu_0$  were plotted against the inhibitor (RM) concentration in Figure 1, where  $\mu_i$  is the “inhibited” growth rate in the presence of RM and  $\mu_0$  is the growth rate of the control culture without RM.

In cases where the increase of RM concentration clearly affected the

growth rate (Figure 1 a, b, c, d, e, f, g, h, and i), the half-maximal inhibitor concentration (IC50) could be determined (Figure S7). The found IC50 values, the RM concentrations that had no or minimal effect on cell growth and the highest tested concentration that still allowed decent growth are summarised in Table 1.

### 3.2. Mediated anodic respiration in a BES reactor

The RMs FEC, DCIP, HNQ, and PMS, were selected for anodic respiration of *C. necator* in the following BES experiments, covering a wide range of redox potentials from  $E_m = -137$  mV (HNQ) to 416 mV (FEC). An interaction of *C. necator* with HNQ would provide valuable insight into the lower limit of redox potentials that a mediator can possess to still accept electrons from the organism. FEC, on the other hand, is a promising artificial RM that is frequently used with gram-negative bacteria [15,39]. Phenazines are often used as natural RMs [14,40] and can be produced by the cells within the BES. DCIP has a very high affinity for organic phases [29], which should promote membrane permeability. Here, 15 mM FEC was used to maximize availability of shuttle molecules without inhibiting *C. necator* too much (Table 1). A similar principle was used with PMS (390  $\mu\text{M}$ ), and HNQ (1.25 mM). DCIP was used at a concentration of 80  $\mu\text{M}$ , at which biocompatibility should be ensured.

Fig. 2 (a) shows the current densities recorded with the 4 different mediators over the entire BES experiment. After inoculation with the *C. necator* preculture at  $t = 0$  h, the current density showed an immediate increase. The maximum current density achieved with FEC surpassed that of the other RMs by 10-fold, reaching 260.75  $\mu\text{A cm}^{-2}$  after 15.8 h. In comparison, DCIP resulted in a maximum current density of 21.67  $\mu\text{A cm}^{-2}$ , while PMS delivered 12.14  $\mu\text{A cm}^{-2}$ , and HNQ 28.85  $\mu\text{A cm}^{-2}$ . With FEC, DCIP, and PMS, the current density peaked at about 24 h, which subsequently decreased significantly. In the case of PMS, the current density eventually returned to the abiotic baseline level after approximately 124 h. In contrast, a stable current density was achieved with HNQ throughout the cultivation period.

Anodic current from HNQ was not expected due to the low  $E_m$  of  $-137$  mV of the mediator. Comparison with the redox potentials of potential molecular interaction sites for the RM suggests that HNQ can accept electrons directly from NADH ( $E_m = -320$  mV), FMN/FAD ( $E_m = -219$  mV), or periplasmic hydrogenases ( $E_m = -414$  mV for the reaction  $\text{H}_2 \rightarrow 2\text{H}^+ + 2\text{e}^-$ ), whereas menaquinone and ubiquinone have higher  $E_m$  of  $-74$  and  $90$  mV, respectively [41,42]. However, it is not yet clear whether HNQ can penetrate the outer and even the cytoplasmic membrane to reach NADH as a reaction partner. For the Gram-positive *Staphylococcus aureus*, unmodified HNQ was shown not to alter the membrane integrity. Furthermore, the calculated  $\log P$  values between 1.2 and  $-1.7$  indicate that HNQ is not very lipophilic, implying that membrane transfer is less likely to occur [43]. Consequently, periplasmic interaction sites accessible through outer membrane porins are most likely the target of HNQ. Among these, membrane bound [NiFe]-hydrogenase (MBH) and respiratory chain complexes (ranging from  $-320$  to  $820$  mV) are possible interaction partners in terms of their redox potentials. The nitrate respiration pathway can be ruled out due to the high redox potential of 420 mV for the nitrate/nitrite couple [44]. At this potential, however, FEC ( $E_m = 416$  mV) could interact with nitrate reductase. This could also explain why the highest current density is obtained with FEC, as this mediator may also interact with other components of the respiratory chain(s) in addition to nitrate reductase. It should also be noted that *C. necator* may not synthesize the nitrate respiration machinery until later in the experiment since the preculture for inoculation was grown aerobically. Nevertheless, the possibility of multiple interaction sites could be crucial for FEC to achieve high current densities due to its relatively high redox potential in combination with its high solubility.

DCIP and PMS are likely to be membrane permeable due to their lipophilic properties [29,45]. The corresponding interaction could be

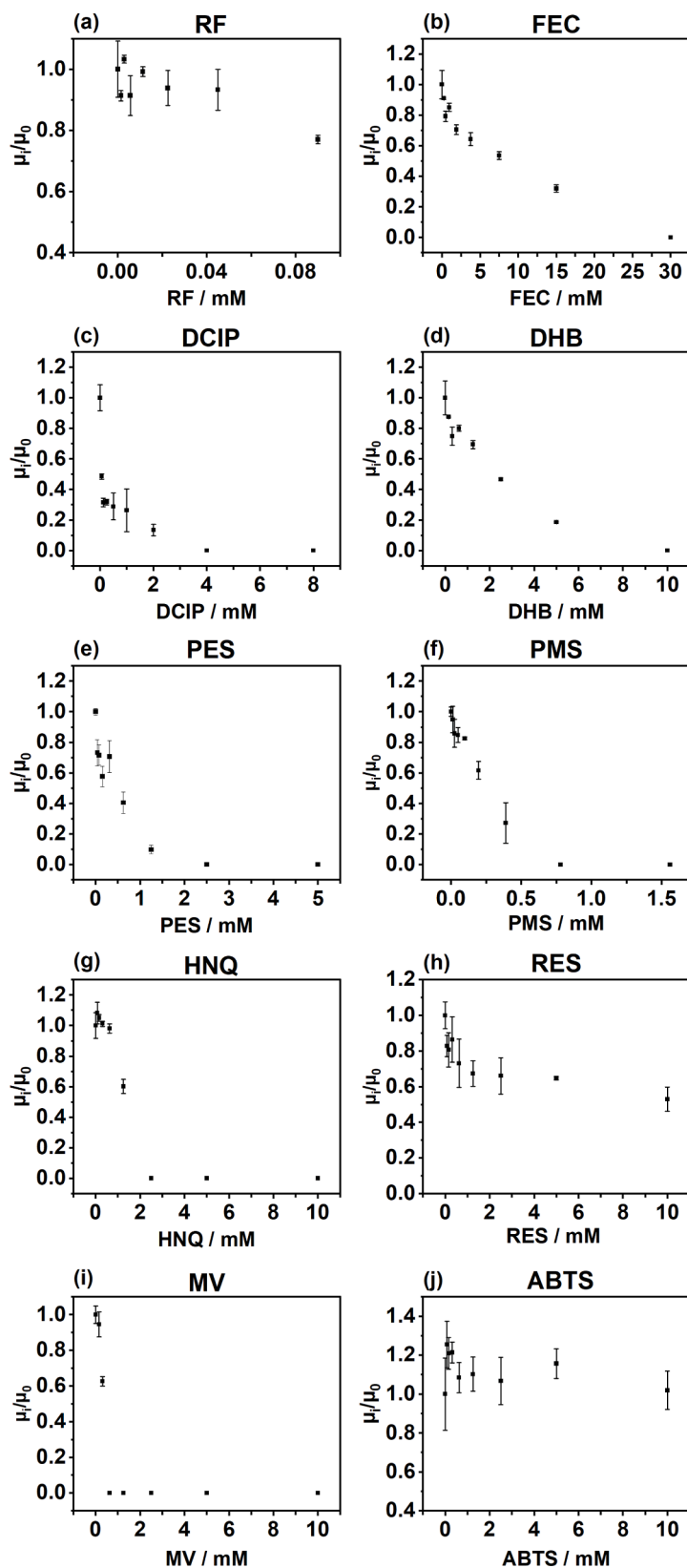


**Fig. 1.** Analysis of different RMs for their inhibitory effects on *C. necator* growth rates. The relative growth rate  $\mu_i/\mu_0$  is plotted vs. RM concentration. *C. necator* was cultivated in minimal medium in the presence or absence of each RM. The corresponding growth curves are depicted in Figure S3. The redox mediators employed were (a) riboflavin (RF), (b) ferricyanide (FEC), (c) 2,6-dichloroindophenole (DCIP), (d) 3,4-dihydroxybenzaldehyde (DHB), (e) phenazine ethosulfate (PES), (f) phenazine methosulfate (PMS), (g) 2-hydroxynaphthaquinone (HNQ), (h) resazurin (RES), (i) methyl viologen (MV), and (j) 2,2'-azino-bis(3-ethylbenzothiazoline-6-sulfonic acid) (ABTS).

**Table 1**

Mediator concentrations with (A) minimal impact on cell growth, (B) the highest tolerated mediator concentrations, and (C) values of IC50.

Redox mediator	A		B		C
	RM <sup>a</sup> [mM]	Growth rate <sup>c,d</sup> [h <sup>-1</sup> ]	RM <sup>b</sup> [mM]	Growth rate <sup>c,d</sup> [h <sup>-1</sup> ]	IC50 [mM]
Methyl viologen (MV)	0.156	0.247	0.313	0.163	0.33
Riboflavin (RF)	0.045	0.281	0.090	0.232	184.30
2-hydroxy-1,4-naphthaquinone (HNQ)	0.313	0.257	1.25	0.153	1.32
Methylene blue (MB) <sup>e,f</sup>	ND	ND	ND	ND	ND
Resazurin (RES)	0.313	0.237	10	0.144	54.21
Phenazine ethosulfate (PES)	0.040	0.235	1.25	0.032	0.28
Phenazine methosulfate (PMS)	0.025	0.200	0.390	0.063	0.22
2,6-dichloroindophenole (DCIP)	0.063	0.119	2	0.033	0.05
3,4-dihydroxybenzaldehyde (DHB)	0.625	0.225	5	0.052	1.83
Ferricyanide (FEC)	0.470	0.239	15	0.096	5.70
2,2'-azino-bis(3-ethylbenzothiazoline-6-sulfonic acid) (ABTS) <sup>f</sup>	5	0.214	10	0.189	ND

<sup>a</sup> RM concentrations at which the impact on cell growth was minimal. The qualitative evaluation is based on the similarity between mediator-containing cultures and control cultures for growth rate, lag phase, and the rate of reaching the stationary phase.

<sup>b</sup> RM concentrations relevant for the BES experiments where *C. necator* cells are used that are in the stationary phase, cell growth is not to be expected, and high RM concentrations allow efficient electron transfer between the cells and the anode.

<sup>c</sup> The average growth rate of the control cultures without RM was  $0.252 \pm 0.046 \text{ h}^{-1}$ .

<sup>d</sup> The mean of three individual measurements is given ( $n = 3$ ).

<sup>e</sup> The growth rates in the presence of MB could not be determined (ND – not determined, see text for details).

<sup>f</sup> The IC50 could not be determined (ND – not determined, see text for details).

anything below the  $E_m$  of DCIP/PMS. Studies with *Dehalococcoides ethenogenes* have suggested a possible interaction of PMS with the periplasmic hydrogenase [46], whereas in the case of *Saccharomyces cerevisiae* and *S. aureus* an interaction of DCIP with complex III and I of the respiratory chain has been proposed [45,47]. The obtained current density curves indicate that the overall electron transfer to the anode lags well behind that of FEC (Fig. 2 (a)). Nevertheless, the reduction of DCIP within the reactor could even be observed visually. When the cells were added to the reactor, the colour of DCIP changed from an intense blue to colourless, indicating its reduction by the cells (Figure S8). This observation hints to a possible limitation in the re-oxidation of DCIP by the anode. The use of different anode materials in future experiments could improve the interaction of mediator and anode.

The coulombic efficiency (CE) was calculated to determine the percentage of electrons transferred from the electron donor fructose to the anode (electron acceptor). A CE of 64.1 % for FEC (Table S1) indicates that 64.1 % of the available electrons from fructose were transferred to the anode. In contrast, only 11.9 % of the available electrons were transferred with HNQ. For DCIP and PMS, the fructose consumption was too low to reliably determine CEs. The remaining percentage of released electrons in the FEC and HNQ reactors that were not transferred to the anode can be attributed to undetermined metabolites on the one hand, and possible biomass accumulation in the first hours after inoculation on the other (Fig. 2 (b)). The reduced mediator molecules present in the medium, which have not yet been reoxidized at the end of cultivation, represent a further electron sink. A periplasmic sugar oxidation pathway, as reported for *P. putida* [15], is not known for *C. necator* and can therefore not be used as the cause of the high CE.

Our results show, that of the 4 RMs compared, anodic respiration of *C. necator* was most efficient with FEC, as it diverts the highest percentage of electrons to the anode. Thus, if the objective is to produce an oxidized product through unbalanced fermentation, similar to what was done previously for acetoin by *S. oneidensis* [48], FEC might be a preferable choice rather than HNQ. In contrast, the latter might offer a better option for production of reduced compounds as more electrons are available for metabolism.

Fructose consumption (Fig. 2 (c)) clearly indicates that *C. necator* showed detectable metabolic activity within the anaerobic BES only with FEC and HNQ. In contrast, *C. necator* did not show significant fructose consumption with either PMS or DCIP. Instead, the fructose concentration slightly increased, possibly as a result of evaporation with

a determined rate of  $0.15 \text{ mL h}^{-1}$ . However, even with FEC and HNQ, the fructose uptake rate was low over 195 h of cultivation. Within the first 24 h, the highest uptake rate was  $4.42$  and  $3.72 \text{ mg L}^{-1} \text{ h}^{-1}$  for FEC and HNQ, respectively. Between 24 and 96 h, the rates decreased to  $2.81$  and  $1.53 \text{ mg L}^{-1} \text{ h}^{-1}$ , respectively, until the rates for both RMs were less than  $0.67 \text{ mg L}^{-1} \text{ h}^{-1}$  after 120 h (Figure S9).

Simultaneously with the increase in current density, the cathodic pH in the reactor with FEC shifted to more basic values. This shift is a consequence of the intense proton consumption caused by the cathodic hydrogen evolution reaction (Fig. 2 (d)). Theoretically, oxygen reduction would be thermodynamically more favourable at the cathode, but due to the lack of stirring in the cathode compartment, oxygen transfer to the cathode was diffusion-limited. It is therefore conceivable that the cathodic pH limits the electrochemical reaction, since a large pH difference between anodic- and cathodic electrolyte lowers the cell voltage according to the Nernst equation [49]. However, a limited re-oxidation of FEC due to an increased cell potential was not observed in our experiment. The opposite was the case, since the mediator was constantly oxidized at the anode (Fig. 3 (a)). Therefore, the cathode reaction probably did not limit the process of anodic respiration with FEC as mediator. However, the reason why the anodic current was restricted to  $260.75 \mu\text{A cm}^{-2}$  after 12 h of cultivation remains unclear. The most plausible explanation might be found on the genomic level, since no obvious limitation in the electrochemical setup was observed. This indicates that the observed anodic electron discharge is not able to replace oxygen as electron acceptor to enable growth.

The cell density was recorded during the cultivation by OD<sub>600</sub> measurements. As DCIP has an absorption maximum at 607 nm, OD<sub>700</sub> was used in this particular case. From Fig. 2 (b) it can be recognized that the cell density of the FEC culture slightly increases in the phase of increase of the current density and showed a downward trend after 48 h. This downward trend was also observed for the PMS and HNQ cultures, while the DCIP culture showed a stable cell density. It should be noted that these results are based on single reactor runs, which does not allow statistical conclusions to be drawn. After cultivation, planktonic cells were harvested, dried, and the resulting dry weight confirmed the optical density data, indicating that the FEC reactor ended up with significantly less biomass compared to the other reactors (Table S1). One reason for this might be that the cells aggregated and attached between the cathode compartment lid and the reactor wall (Figure S10).

Since RMs were introduced into the medium at different

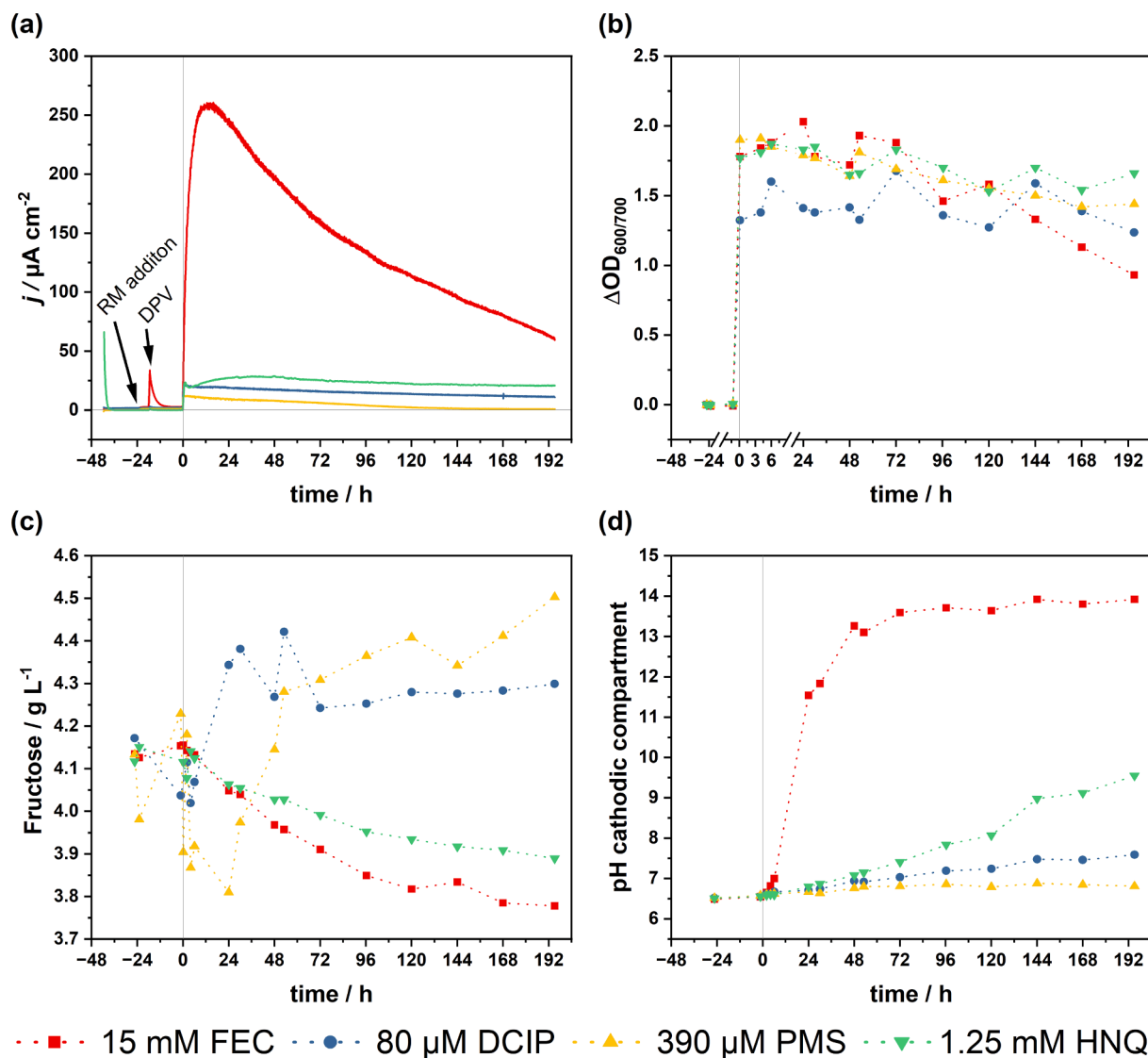


Fig. 2. Anodic respiration of *C. necator* with FEC (red), DCIP (blue), PMS (yellow), and HNQ (green) as mediators. (a) Current density during fermentation. The addition of FEC and PMS as well as the DPV measurement, which resulted in a current peak in the chronoamperometric measurement, are marked by arrows. (b) Cell density determined by OD measurement. (c) Fructose concentration determined by HPLC. (d) pH values in the cathodic compartment. Conditions: Applied anodic potential: FEC, 697 mV; DCIP, 497 mV; PMS, 297 mV; HNQ, 197 mV. 300 mL minimal medium made anaerobic through flushing the headspace with  $45 \text{ mL min}^{-1} \text{ N}_2$ , 400 rpm,  $30^\circ\text{C}$ ,  $n = 1$ . The inoculate was added at  $t = 0$  h time.

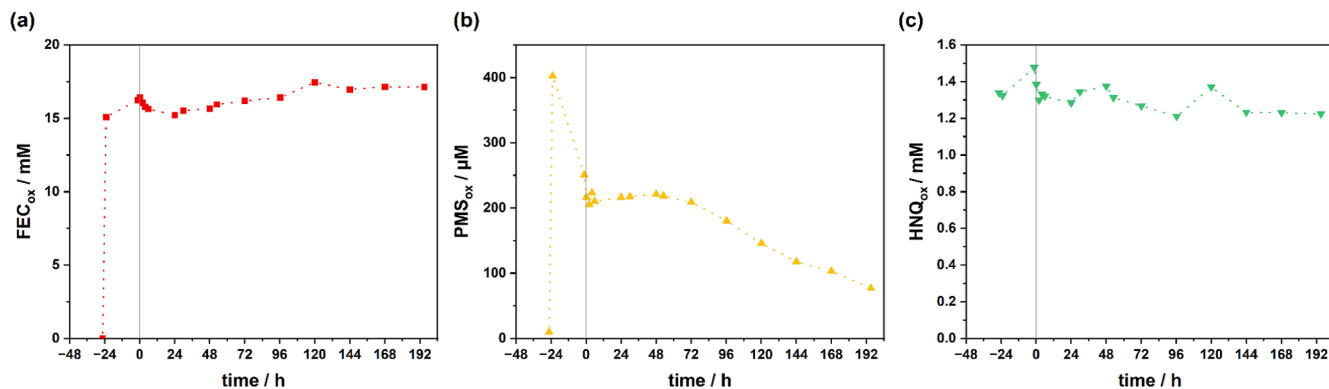


Fig. 3. Concentrations of oxidized RMs during BES cultivation. Culture samples were withdrawn at different time points, centrifuged, and the concentrations of oxidized (a) FEC, (b) PMS, and (c) HNQ in the supernatant were determined spectrophotometrically. FEC and PMS were added 24 h prior to inoculation. Wavelengths: 320/420 nm (FEC), 383 nm (PMS), 452 nm (HNQ). The inoculate was added at  $t = 0$  h time.

concentrations, the calculation of the total turnover number (TTN) provides an opportunity to compare their performance independent of their concentration. After 195 h of cultivation, the TTN was 4.18 for FEC, 41.04 for DCIP, 2.62 for PMS, and 4.13 for HNQ. The total concentration of the individual RMs is taken into account when calculating the TTN. DCIP therefore shows a very high TTN, although the resulting current is comparably low. Interestingly, HNQ achieved the same number of turnovers as FEC even though it was added in a 12-fold lower concentration. However, it is important to consider that not every mediator molecule is constantly shuttling electrons back and forth between the microbe and the electrode. Accordingly, in the case of FEC, it might be possible to use a lower mediator concentration if only a fraction of the RM molecules is reduced by the cells. Optimization of electron transfer efficiency by lowering the mediator concentration should be considered in future experiments.

By utilising the characteristic wavelengths of the oxidized RMs, quantitative offline measurements of the RM pool were conducted during the BES experiments. Cell-free samples were prepared from the reactors and measured spectrophotometrically. Fig. 3 depicts the resulting concentration curves for FEC, PMS, and HNQ. The redox state of the DCIP pool could not be measured with the available equipment, as it re-oxidizes immediately upon contact with air. Reduced PMS is also known to re-oxidize in contact with O<sub>2</sub> at a rate constant of about 180 M<sup>-1</sup>s<sup>-1</sup> to form the semiquinone, which increases the absorbance at 387 and 440 nm [50]. The subsequent oxidation to fully oxidized PMS proceeds more slowly and shifts the absorbance maximum to 387 nm [51]. The photometric measurement is therefore prone to error and can only show a trend of the oxidation state present in the reactor. Furthermore, PMS is known to decompose upon illumination under anaerobic conditions in equal amounts to reduced PMS and pyocyanine. Pyocyanine can be detected photometrically due to its absorption maximum of about 310 nm [50]. The experimental data show that the absorption at 311 nm indeed increased slightly after the cells were added to the system (Figure S11), suggesting that some degradation occurred even though the reactors were protected from light. The initial RM concentrations determined by absorption measurements, showed slight deviations from the calculated initial concentrations (Fig. 3). One partial reason for this might be the inaccuracy that comes with adding the RMs to the reactors with syringes.

In the case of FEC, after an initial decrease shortly after inoculation, the amount of oxidized FEC steadily increased, even beyond the amount initially added. Reasons for this can only be speculated. Again, a possible factor includes a concentration effect due to evaporation in the reactor. Another possibility might be the accumulation of metabolites in the medium with similar absorption as FEC, which were not detectable with the applied HPLC method. Further investigations are required to understand the reasons for this observation. Nevertheless, the results clearly show that FEC is efficiently re-oxidized at the electrode and thus the availability of oxidized mediator molecules does not limit the overall process. The amount of oxidized HNQ appeared to increase in the first abiotic polarisation phase. This might be due to residual reduced HNQ being oxidized at the anode. After inoculation, the concentration of oxidized HNQ first decreased slightly and then increased again to approximately 1.35 mM after 30 h. Consequently, the concentration of oxidized HNQ remained relatively stable, hovering around 1.25 mM, taking into account the variations of the method. This might imply that only a fraction of the FEC and HNQ pools was reduced by the cells and most of the available mediator molecules remained in the oxidized state. However, it is more likely that the anode re-oxidized the RMs at a relatively high rate, which contributes to the observed concentration patterns. In contrast, PMS appeared to be reduced or degraded in the abiotic phase, the latter being more plausible because of the oxidizing potential applied to the medium and because of the known degradation reaction discussed above. However, pyocyanine was most likely not formed in this reaction, since the absorption at 311 nm remained almost constant in the abiotic phase (Figure S11). After inoculation, the

concentration of oxidized PMS appeared to stabilize until it dropped again after 72 h. At the end of the experiment, only 77 μM of oxidized PMS remained.

### 3.3. Electrochemical mediator analysis by DPV

For electrochemical characterization of the RMs during the BES cultivation, DPV (differential pulse voltammetry) measurements were conducted instead of conventional cyclic voltammetry because the former is less susceptible to capacitive currents. Comparison of DPV scans of HNQ and FEC (Fig. 4 (a,d)) in the abiotic and post-biotic phases revealed no significant changes in potential and peak current. Together with the concentrations measured via absorption and the constant current density, it can be concluded that HNQ and FEC are very stable RMs under the applied conditions.

From the current density curve and the spectrophotometric concentration measurement it can be deduced that PMS is not stable over longer time periods, as has already been described for aqueous PMS solutions [52]. The DPV measurements indicate a side reaction of PMS in the BES reactor, as illustrated by a prominent secondary peak at -127 mV in the voltammogram after 195 h of cultivation (Fig. 4 (c)). In contrast, only a single peak at 90 mV was visible for PMS in the abiotic phase. Remarkably, the total peak current did not decrease significantly, although PMS was already degraded/reduced in the first abiotic 24 h according to the absorption measurements. According to DPV, no secondary peak formed during this time period. As discussed before, the anaerobic photodegradation of PMS to pyocyanine is expected to some extent. However, the redox potential of pyocyanine is reported to be -60 mV [26]. Therefore, another degradation product might be present in the solution. Heterologous production of a biological phenazine mediator might therefore be a preferable option for continuous supply of the RM, as previously shown for *P. putida* KT2440 [14].

The DCIP-added culture showed a significantly decreased peak current after 195 h compared to the abiotic phase, indicating a decrease in the amount of electrochemically active molecules in the system, as peak currents correlate with the concentration of the RM (Fig. 4 (b)) [53,54]. This could be due to either RM accumulation within the cells or degradation. Therefore, DCIP may not be suitable for use as the sole mediator over long time periods, but its high TTN could still be useful when combined with a secondary mediator to support electron transfer to the cytoplasmic membrane.

## 4. Conclusions

Analysis of the inhibitory effect of redox mediators on *C. necator* cell cultures revealed that the higher the initial cell density, the higher the permissible concentration of redox mediators. In case of *C. necator*, FEC, ABTS, and RES are the redox mediators that can be used in larger amounts. However, in some instances, the limited solubility of the RM does not allow for higher concentrations, preventing an adequate analysis of their inhibitory effect.

According to our BES data, FEC appears to be the most promising redox mediator for anodic respiration by *C. necator*. It is stable during the fermentation process, can be used at concentrations up to 15 mM without having a significant inhibitory effect, when stationary cells are used. Furthermore, it does not appear to limit the electrochemical reaction. A stable but low anodic current was achieved with HNQ, which was not to be expected due to its low  $E_m$ . As already hypothesized for *P. putida*, the high charge and hydrophilic character of the [Fe(CN)<sub>6</sub>]<sup>3-</sup> molecule most likely prohibits FEC to penetrate the hydrophobic cytoplasmic membrane. Therefore, a possible interaction with periplasmic electron transferring proteins is most likely. The same applies to HNQ until its ability to penetrate the cytoplasmic membrane is demonstrated. PMS and DCIP provided only low current densities, although they have been shown to pass bacterial membranes. However, the lack of fructose consumption of the *C. necator* cultures with PMS and DCIP indicates that

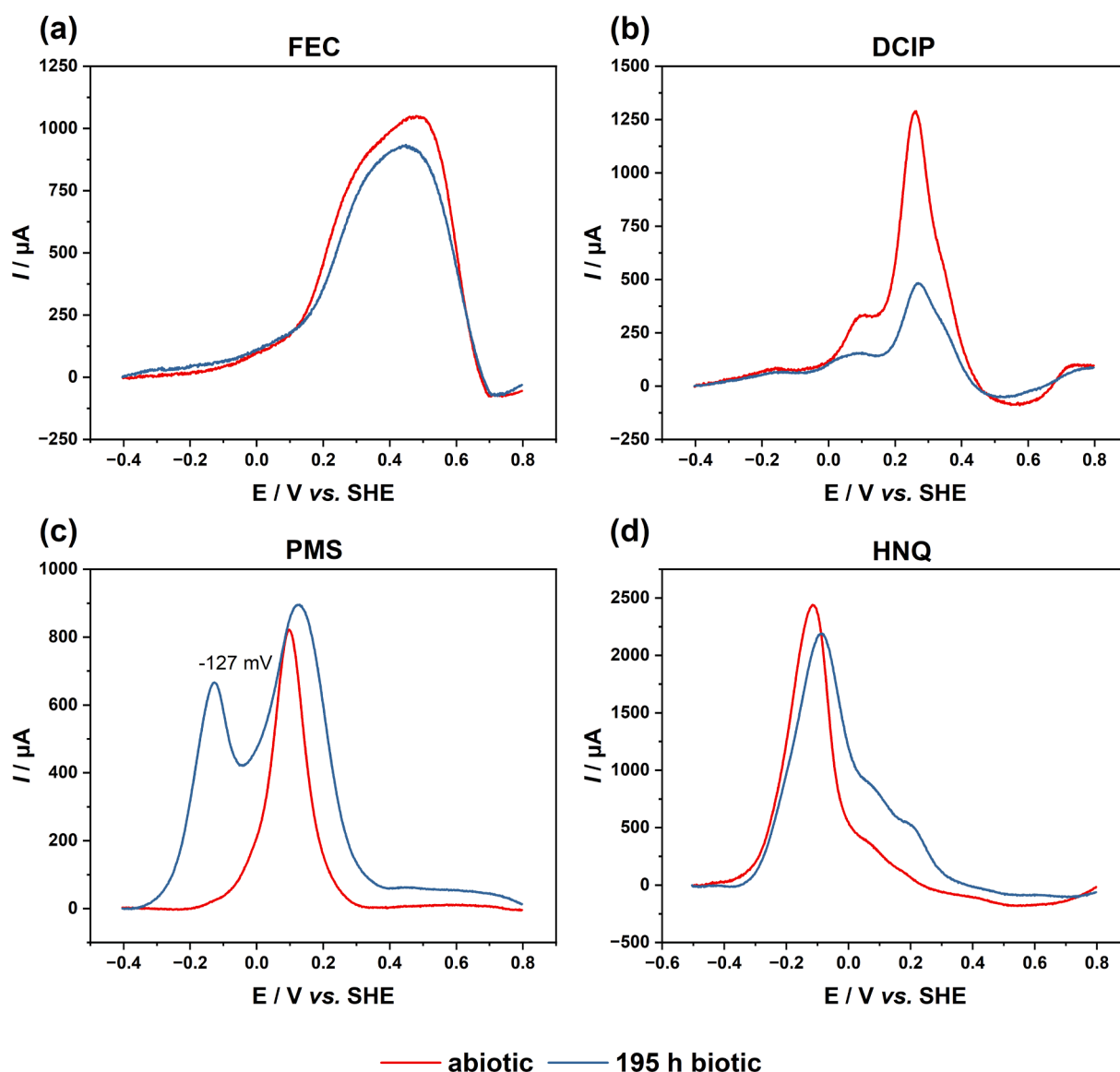


**Fig. 4.** DPV analysis of the four RMs used in the BES. Measurements were conducted for (a) FEC, (b) DCIP, (c) PMS, and (d) HNQ in the abiotic polarisation phase (red traces) and after 195 h of cultivation (blue traces). The baseline is normalised to an initial current of 0 mA.

neither RM is suitable for BES, and in case of PMS, additional problems arise from constant degradation. Future experiments combining FEC with a redox-compatible RM that can cross the cytoplasmic membrane may even increase the EET capabilities of *C. necator* to achieve 100 % substitution of  $O_2$ .

#### CRedit authorship contribution statement

**André Gemünde:** Writing – original draft, Visualization, Methodology, Investigation, Data curation. **Elena Rossini:** Writing – original draft, Visualization, Methodology, Investigation, Data curation. **Oliver Lenz:** Writing – review & editing, Project administration, Funding acquisition. **Stefan Frielingsdorf:** Writing – review & editing, Supervision, Project administration, Funding acquisition, Conceptualization. **Dirk Holtmann:** Writing – review & editing, Supervision, Project administration, Funding acquisition, Conceptualization.

#### Declaration of competing interest

The authors declare that they have no known competing financial interests or personal relationships that could have appeared to influence

the work reported in this paper.

#### Data availability

Data will be made available on request.

#### Acknowledgements

This work was created as part of the project “Bioelectrochemical and engineering fundamentals to establish electro-biotechnology for biosynthesis – Power to value-added products (eBiotech)”, which is funded by the Deutsche Forschungsgemeinschaft (DFG, German Research Foundation) – Project number 422694804. Furthermore, this work was funded by the DFG under Germany’s Excellence Strategy – EXC 2008 – 390540038 – UniSysCat.

#### Appendix A. Supplementary data

Supplementary data to this article can be found online at <https://doi.org/10.1016/j.bioelechem.2024.108694>.

## References

- [1] P. Aelterman, K. Rabaey, P. Clauwaert, W. Verstraete, Microbial fuel cells for wastewater treatment, *water sci. technol.: j. Int. Assoc. Water Pollut. Res.* 54 (2006) 9–15.
- [2] R.M. Alonso, M.I. San-Martín, R. Mateos, A. Morán, A. Escapa, Scale-up of bioelectrochemical systems for energy valorization of waste streams, in: *Microbial Electrochemical Technologies*, CRC Press, 2020, pp. 447–459.
- [3] R. Rossi, A.Y. Hur, M.A. Page, A.O. Thomas, J.J. Butkiewicz, D.W. Jones, G. Baek, P.E. Saikaly, D.M. Crotek, B.E. Logan, Pilot scale microbial fuel cells using air cathodes for producing electricity while treating wastewater, *Water Res.* 215 (2022) 118208.
- [4] H. Wohlers, L. Assil-Companioni, D. Holtmann, Chapter 11 cupriavidus necator – a broadly applicable aerobic hydrogen-oxidizing bacterium, in: R. Kourist, S. Schmidt (Eds.), *The Autotrophic Biorefinery: Raw Materials from Biotechnology*, De Gruyter, 2021, pp. 297–318.
- [5] T. Krieg, A. Sydow, S. Faust, I. Huth, D. Holtmann, CO<sub>2</sub> to terpenes: autotrophic and electroautotrophic  $\alpha$ -humulene production with cupriavidus necator, *Angew. Chem. Int. Ed. Engl.* 57 (2018) 1879–1882.
- [6] R.R. Dalsasso, F.A. Pavan, S.E. Bordignon, G.M.F. de Aragão, P. Poletto, Polyhydroxybutyrate (PHB) production by cupriavidus necator from sugarcane vinasse and molasses as mixed substrate, *Process Biochem.* 85 (2019) 12–18.
- [7] J. Panich, B. Fong, S.W. Singer, Metabolic engineering of cupriavidus necator H16 for sustainable biofuels from CO<sub>2</sub>, *Trends Biotechnol.* 39 (2021) 412–424.
- [8] O. Lenz, L. Lauterbach, S. Frielingsdorf, Chapter five - O<sub>2</sub>-tolerant [NiFe]-hydrogenases of ralstonia eutropha H16: physiology, molecular biology, purification, and biochemical analysis, in: F. Armstrong (Ed.), *Methods in Enzymology Enzymes of Energy Technology*, Academic Press, 2018, pp. 117–151.
- [9] A. Gemünde, J. Gail, D. Holtmann, Anodic respiration of Vibrio natriegens in a bioelectrochemical system, *ChemSusChem* (2023) e202300181.
- [10] I. Vassilev, N.J.H. Aversch, P. Ledezma, M. Kokko, Anodic electro-fermentation: empowering anaerobic production processes via anodic respiration, *Biotechnol. Adv.* 107728 (2021).
- [11] L. Gu, X. Xiao, S. Yup Lee, B. Lai, C. Solem, Superior anodic electro-fermentation by enhancing capacity for extracellular electron transfer, *Bioresour. Technol.* 389 (2023) 129813.
- [12] L. Shi, D.J. Richardson, Z. Wang, S.N. Kerisit, K.M. Rosso, J.M. Zachara, J. K. Fredrickson, The roles of outer membrane cytochromes of shewanella and geobacter in extracellular electron transfer, *Environ. Microbiol. Rep.* 1 (2009) 220–227.
- [13] G. Reguera, K.D. McCarthy, T. Mehta, J.S. Nicoll, M.T. Tuominen, D.R. Lovley, Extracellular electron transfer via microbial nanowires, *Nature* 435 (2005) 1098–1101.
- [14] S. Schmitz, S. Nies, N. Wierckx, L.M. Blank, M.A. Rosenbaum, Engineering mediator-based electroactivity in the obligate aerobic bacterium Pseudomonas putida KT2440, *Front. Microbiol.* 6 (2015) 284.
- [15] B. Lai, S. Yu, P.V. Bernhardt, K. Rabaey, B. Virdis, J.O. Krömer, Anoxic metabolism and biochemical production in Pseudomonas putida F1 driven by a bioelectrochemical system, *Biotechnol. Biofuels* 9 (2016) 39.
- [16] A. Gemünde, B. Lai, L. Pause, J. Krömer, D. Holtmann, Redox mediators in microbial electrochemical systems, *ChemElectroChem* (2022).
- [17] K. Nishio, Y. Kimoto, J. Song, T. Konno, K. Ishihara, S. Kato, K. Hashimoto, S. Nakanishi, Extracellular electron transfer enhances polyhydroxybutyrate production in ralstonia eutropha, *Environ. Sci. Technol. Lett.* 1 (2014) 40–43.
- [18] Y.H. Lai, J.-C.-W. Lan, Enhanced polyhydroxybutyrate production through incorporation of a hydrogen fuel cell and electro-fermentation system, *Int. J. Hydrogen Energy* 46 (2021) 16787–16800.
- [19] P.A. Davison, W. Tu, J. Xu, S. Della Valle, I.P. Thompson, C.N. Hunter, W.E. Huang, Engineering a rhodopsin-based photo-Electrosynthetic system in bacteria for CO<sub>2</sub> fixation, *ACS Synth. Biol.* 11 (2022) 3805–3816.
- [20] W. Tu, J. Xu, I.P. Thompson, W.E. Huang, Engineering artificial photosynthesis based on rhodopsin for CO<sub>2</sub> fixation, *Nat Commun* 14 (2023) 8012.
- [21] B. Myers, F. Catrambone, S. Allen, P.J. Hill, K. Kovacs, F.J. Rawson, Engineering nanowires in bacteria to elucidate electron transport structural-functional relationships, *Sci. Rep.* 13 (2023) 8843.
- [22] M.A.D. de Rienzo, I.M. Banat, B. Dolman, J. Winterburn, P.J. Martin, Sophorolipid biosurfactants: possible uses as antibacterial and antibiofilm agent, *N. Biotechnol.* 32 (2015) 720–726.
- [23] C. Liu, T. Sun, Y. Zhai, S. Dong, Evaluation of ferricyanide effects on microorganisms with multi-methods, *Talanta* 78 (2009) 613–617.
- [24] O. Simoska, E.M. Gaffney, K. Lim, K. Beaver, S.D. Minter, Understanding the properties of phenazine mediators that promote extracellular electron transfer in Escherichia coli, *J. Electrochem. Soc.* 168 (2021) 25503.
- [25] H.G. Schlegel, R. Lafferty, I. Kraus, The isolation of mutants not accumulating poly-beta-hydroxybutyric acid, *Arch. Mikrobiol.* 71 (1970) 283–294.
- [26] M.L. Fultz, R.A. Durst, Mediator compounds for the electrochemical study of biological redox systems: a compilation, *Anal. Chim. Acta* 140 (1982) 1–18.
- [27] D.H. Park, J.G. Zeikus, Utilization of electrically reduced neutral red by actinobacillus succinogenes: physiological function of neutral red in membrane-driven fumarate reduction and energy conservation, *J. Bacteriol.* 181 (1999) 2403–2410.
- [28] A.H. Förster, S. Beblawy, F. Golitsch, J. Gescher, Electrode-assisted acetoin production in a metabolically engineered Escherichia coli strain, *Biotechnol. Biofuels* 10 (2017) 65.
- [29] F.J. Rawson, A.J. Downard, K.H. Baronian, Electrochemical detection of intracellular and cell membrane redox systems in Saccharomyces cerevisiae, *Sci. Rep.* 4 (2014) 5216.
- [30] A. Sydow, T. Krieg, R. Ulber, D. Holtmann, Growth medium and electrolyte-how to combine the different requirements on the reaction solution in bioelectrochemical systems using cupriavidus necator, *Eng. Life Sci.* 17 (2017) 781–791.
- [31] J.L. Sebaugh, Guidelines for accurate EC50/IC50 estimation, *Pharm. Stat.* 10 (2011) 128–134.
- [32] K. Liu, Y. Luo, L. Hao, J. Chen, Antimicrobial effect of methylene blue in microbiologic culture to diagnose periprosthetic joint infection: an in vitro study, *J Orthop Surg Res* 17 (2022) 571.
- [33] M.A. Thirumurthy, A.K. Jones, Geobacter cytochrome OmcZs binds riboflavin: implications for extracellular electron transfer, *Nanotechnology* 31 (2020) 124001.
- [34] V. Ponti, M.U. Dianzani, K. Cheeseman, T.F. Slater, Studies on the reduction of nitroblue tetrazolium chloride mediated through the action of NADH and phenazine methosulphate, *Chem. Biol. Interact.* 23 (1978) 281–291.
- [35] R. Naumann, D. Mayer, P. Bannasch, Voltammetric measurements of the kinetics of enzymatic reduction of 2, 6-dichlorophenolindophenol in normal and neoplastic hepatocytes using glucose as substrate, *Biochim. Biophys. Acta. Mol. Cell. Res.* 847 (1985) 96–100.
- [36] M. Bahari, M.A. Malmberg, D.M. Brown, S. Hadi Nazari, R.S. Lewis, G.D. Watt, J. N. Harb, Oxidation efficiency of glucose using viologen mediators for glucose fuel cell applications with non-precious anodes, *Appl. Energy* 261 (2020) 114382.
- [37] S.-A. Ong, E. Toorisaka, M. Hirata, T. Hano, Biodegradation of redox dye methylene blue by up-flow anaerobic sludge blanket reactor, *J. Hazard. Mater.* 124 (2005) 88–94.
- [38] U. Schröder, FUEL CELLS – EXPLORATORY FUEL CELLS | microbial fuel cells, in: J. Garche (Ed.), *Encyclopedia of Electrochemical Power Sources*, Elsevier, Amsterdam, 2009, pp. 206–216.
- [39] P. Ertl, B. Unterladstätter, K. Bayer, S.R. Mikkelsen, Ferricyanide reduction by Escherichia coli: kinetics, mechanism, and application to the optimization of recombinant fermentations, *Anal. Chem.* 72 (2000) 4949–4956.
- [40] A. Chukwubikem, C. Berger, A. Mady, M.A. Rosenbaum, Role of phenazine-enzyme physiology for current generation in a bioelectrochemical system, *Microb. Biotechnol.* (2021).
- [41] K.I. Takamiya, P.L. Dutton, Ubiquinone in Rhodospseudomonas sphaeroides. some thermodynamic properties, *Biochim. Biophys. Acta* 546 (1979) 1–16.
- [42] T.D. Harrington, V.N. Tran, A. Mohamed, R. Renslow, S. Biria, L. Orfe, D.R. Call, H. Beyenal, The mechanism of neutral red-mediated microbial electrosynthesis in Escherichia coli: menaquinone reduction, *Bioresour. Technol.* 192 (2015) 689–695.
- [43] R. Song, B. Yu, D. Friedrich, J. Li, H. Shen, H. Krautscheid, S.D. Huang, M.-H. Kim, Naphthoquinone-derivative as a synthetic compound to overcome the antibiotic resistance of methicillin-resistant S. aureus, *Commun. Biol.* 3 (2020) 529.
- [44] B.C. Berks, S.J. Ferguson, J.W. Moir, D.J. Richardson, Enzymes and associated electron transport systems that catalyse the respiratory reduction of nitrogen oxides and oxyanions, *Biochim. Biophys. Acta* 1232 (1995) 97–173.
- [45] R.Y.A. Hassan, U. Wollenberger, Mediated bioelectrochemical system for biosensing the cell viability of Staphylococcus aureus, *Anal. Bioanal. Chem.* 408 (2016) 579–587.
- [46] I. Nijenhuis, S.H. Zinder, Characterization of hydrogenase and reductive dehalogenase activities of dehalococcoides ethenogenes strain 195, *Appl. Environ. Microbiol.* 71 (2005) 1664–1667.
- [47] J. Zhao, Z. Wang, C. Fu, M. Wang, Q. He, The mediated electrochemical method for rapid fermentation ability assessment, *Electroanalysis* 20 (2008) 1587–1592.
- [48] T. Bursac, J.A. Gralnick, J. Gescher, Acetoin production via unbalanced fermentation in shewanella oneidensis, *Biotechnol. Bioeng.* 114 (2017) 1283–1289.
- [49] R.A. Rozendal, H.V.M. Hamelers, R.J. Molenkamp, C.J.N. Buisman, Performance of single chamber biocatalyzed electrolysis with different types of ion exchange membranes, *Water Res.* 41 (2007) 1984–1994.
- [50] F.G. Halaka, G.T. Babcock, J.L. Dye, Properties of 5-methylphenazinium methyl sulfate. reaction of the oxidized form with NADH and of the reduced form with oxygen, *J. Biol. Chem.* 257 (1982) 1458–1461.
- [51] W.S. Zaugg, Spectroscopic Characteristics and some chemical properties of N-methylphenazinium methyl sulfate (phenazine methosulfate) and pyocyanine at the semiquinoid oxidation level, *J. Biol. Chem.* 239 (1964) 3964–3970.
- [52] R. Ghosh, J.R. Quayle, Phenazine ethosulfate as a preferred electron acceptor to phenazine methosulfate in dye-linked enzyme assays, *Anal. Biochem.* 99 (1979) 112–117.
- [53] L.E. Leon, D.T. Sawyer, Simultaneous determination of iron(II) and iron(III) at micromolar concentrations by differential pulse polarography, *Anal. Chem.* 53 (1981) 706–709.
- [54] K.J. Stutts, M.A. Dayton, R.M. Wightman, Integration of differential pulse voltammograms for concentration measurements, *Anal. Chem.* 54 (1982) 995–998.